

Determining the Catalyst Properties That Lead to High Activity and Selectivity for Catalytic Hydrodeoxygénéation with Ruthenium Pincer Complexes

Wenzhi Yao, Sanjit Das, Nicholas A. DeLucia, Fengrui Qu, Chance M. Boudreux, Aaron K. Vannucci,* and Elizabeth T. Papish*



Cite This: <https://dx.doi.org/10.1021/acs.organomet.9b00816>



Read Online

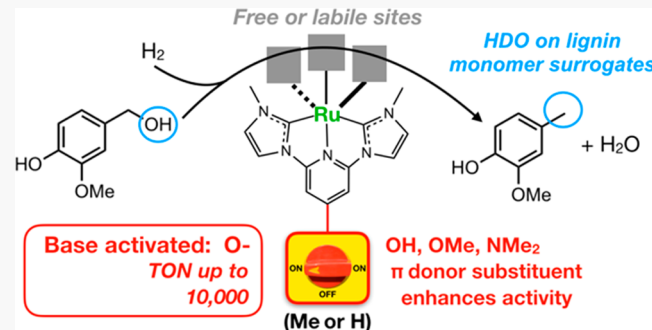
ACCESS |

Metrics & More

Article Recommendations

Supporting Information

ABSTRACT: Ten ruthenium pincer complexes were evaluated as catalysts for the hydrodeoxygénéation (HDO) reaction on a lignin monomer surrogate, vanillyl alcohol. Four of these complexes are reported herein with the synthesis and full characterization data for all and single-crystal X-ray diffraction data for three complexes bearing OH/O⁻, NMe₂, and Me substituents on the pincer. A systematic study of these CNC pincer complexes revealed that the π -donor substituent on the pyridine ring plays a key role in enhancing the yield of the desired deoxygenated product. While OMe, OH, and NMe₂ are all effective as π -donor substituents on the central pyridine ring in the pincer, the highest conversion to products and the best selectivity was observed with OH substituents and added sodium carbonate as a base. Base serves to deprotonate the OH group and form O^- as observed spectroscopically. Furthermore, efforts to use other catalysts have revealed that free or labile sites are needed on the ruthenium center and an electronically rich and nonbulky CNC pincer is optimal. At low catalyst loadings (0.01 mol %), the OH-substituted catalyst I^{OH} in the presence of base serves as a homogeneous catalyst and is able to achieve quantitative and selective conversion of vanillyl alcohol to desired the HDO product, creosol, with up to 10000 turnovers. With this knowledge in hand, we can design the next generation of homogeneous catalysts with increased reactivity toward all of the oxygenated sites on lignin-derived monomers.



INTRODUCTION

Total world energy consumption was 575 quadrillion Btu in 2015, and it is predicted to increase to 736 quadrillion Btu in 2040.¹ In addition, renewable fuels are predicted to be the world's fastest growing energy source, with consumption increasing by an average 2.3% per year between 2015 and 2040. Renewables contributed 19% to the total energy consumption in 2012.² The largest fraction of renewables is traditional biomass, which contributed 9% to the total energy consumption. To convert biomass to a more useful energy form, there are three main thermal processes available: namely, pyrolysis, gasification, and combustion.³ The main product from pyrolysis of biomass is bio-oil. Bio-oil has problems of thermal instability, affinity for water, corrosivity, high viscosity, and low heating values, due to its high oxygen content.⁴ To expand the utility of the bio-oil, selective deoxygenation can be applied to reduce oxygen from the compounds. Furthermore, recent advances in biomass processing and lignin depolymerization have led to a greatly increased need for catalysts capable of selective deoxygenation of aromatic alcohols.^{5–10}

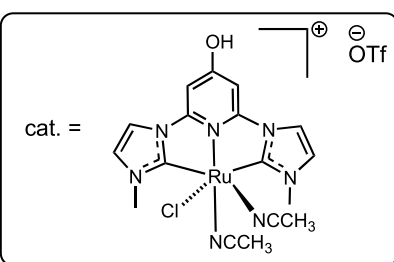
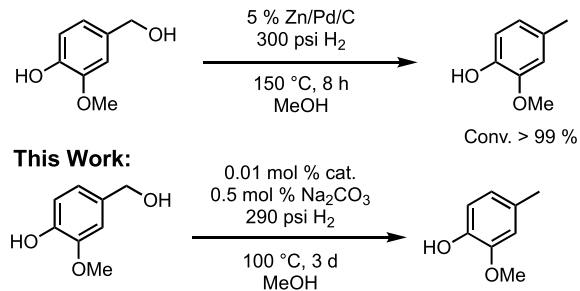
Deoxygenation of the aromatic alcohols would increase the energy density of the resulting liquid fuel¹¹ and/or lead to the

isolation of important industrial chemical feedstocks.¹² Selectively deoxygenating lignin-derived compounds without hydrogenation of the aromatic units is of specific interest because aromatics and alkenes are higher value chemicals in comparison to alkanes, hydrogen use efficiency would be maximized, and carbon loss would be minimized.¹³ Traditional nanoparticle-based heterogeneous catalysts can achieve upward of 80–90% selectivity for the hydrodeoxygénéation of model compounds.^{14–20} Of these model compounds, vanillyl alcohol has been previously studied as a commonly derived chemical from lignin depolymerization. Heterogeneous Pd nanoparticle catalysts have exhibited good product selectivity for the formation of creosol depending on the reaction additives as shown in Scheme 1.^{21–23} Molecular catalysts have also been examined for catalytic HDO of benzylic alcohols due to the fact that molecular catalysts lack extended metallic surfaces and

Received: December 2, 2019

Scheme 1. Hydrodeoxygination of Organic Substrates with Heterogeneous Catalysts and Ruthenium Pincer Catalysts

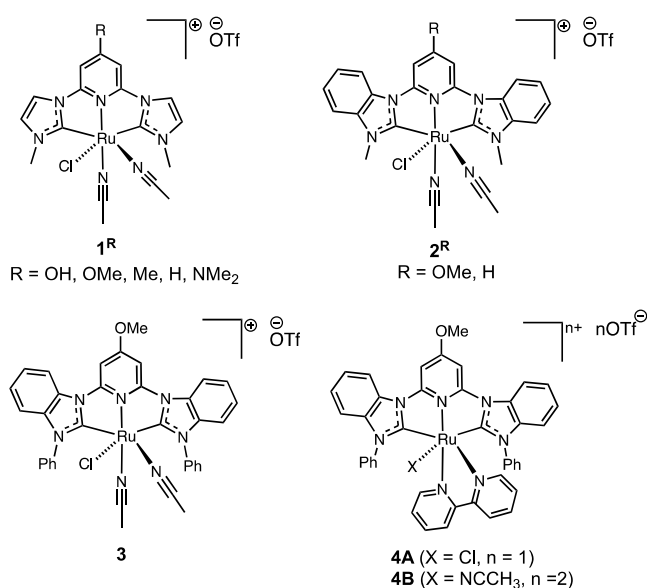
Previous Work:



thus can avoid unwanted ring hydrogenation products.²⁴ A molecular palladium catalyst in homogeneous methanol solution has exhibited complete selectivity for HDO over ring hydrogenation for benzylic substrates,²⁵ and a molecular catalyst attached to the surface of oxide particles has exhibited high selectivity and activity toward the formation of creosol from vanillyl alcohol and vanillin.²⁶

Here we examine the ability of a series of molecular ruthenium catalysts (Scheme 2)^{27–30} to perform selective HDO on vanillyl alcohol. The coordination environment around the Ru center and the electron-donating ability of the catalysts were systematically varied to gain an understanding of the catalyst reactivity and how it depends upon ligand design. The results show that the electron donor strength of the

Scheme 2. Catalyst Structures Tested for Hydrodeoxygination of Organic Substrates



ligands plays an important role in the catalytic activity of these catalysts, and this work thus lays the groundwork for the rational design of future molecular HDO catalysts.

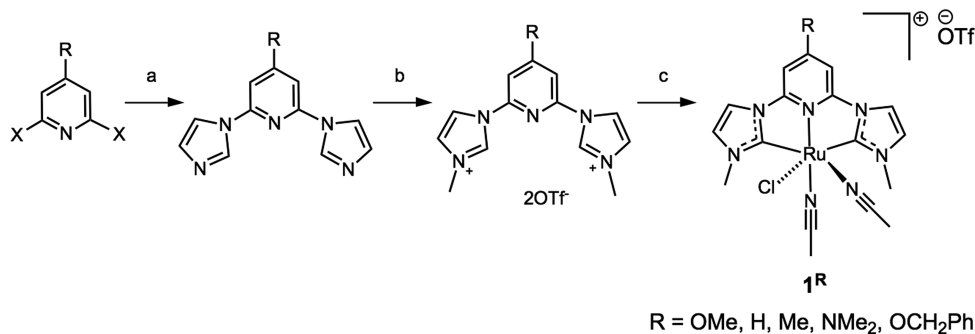
RESULTS AND DISCUSSION

Catalyst Structures. Catalysts of type 1^R (Scheme 2) contain a CNC pincer featuring an imidazole-based NHC ring bonded to a pyridine derivative. The advantage of this class of catalysts is ease of synthetic preparation and ability to vary the R group on the pyridine ring (R) can be OMe or H, as described in our published work,²⁹ or it can be OH, NMe₂, or Me as recently synthesized and characterized herein (further details below and in Scheme 3). For catalysts of type 2^R, the imidazole-based NHC ring is replaced with benzimidazole, which weakens the NHC donor strength.^{27–29,31} Complex 2^H is previously unreported and was characterized by ¹H NMR, ¹³C NMR, ¹⁹F NMR, MS, and IR methods (see the Supporting Information). Catalyst 3 builds upon 2^{OMe} by replacing methyl wingtips with phenyl wingtips on the NHC rings. Catalysts 4A and 4B replace two acetonitrile ligands with a bidentate chelate on ruthenium and were synthesized by adding 2,2'-bipyridine (bipy) to 3 using a multistep route described previously.³⁰ Four of these catalysts (2^{OMe}, 3, 4A,B) were synthesized and characterized in a recent paper on photocatalytic self-sensitized CO₂ reduction to form CO.²⁹ On comparison of some of these catalysts to each other, the donor strength of the pincer (and extent of metal to ligand back-bonding from Ru to NCCN₃ by IR spectroscopy) decreases in the order 1^{OMe} > 2^{OMe} > 3 with the same substituents on Ru and on the pyridine of the pincer. Furthermore, the presence of π-donor R groups (e.g., OH, OMe) results in a more electron rich pincer.

Synthesis of 1^{OH}, 1^{NMe₂}, and 1^{Me}. The pincer ligand precursors were synthesized in two steps by treating 4-R-2,6-dihalopyridine (R = Me, NMe₂) with deprotonated imidazole followed by methylation with methyl triflate. The bis(imidazolium) salt is then treated with base in acetonitrile to generate the free carbene *in situ*, and metalation is achieved with [Ru(*p*-cym)2]₂, leading to complex 1^R (Scheme 3). This procedure has been used previously to form 1^{OMe} and 1^H, but we recently found that using triethylamine as the base (vs Cs₂CO₃) in step c led to a cleaner reaction and an improved yield.

The synthesis of 1^{OH} proved more challenging because NHC ligands are known to be sensitive to protic groups. Thus, the OH functionality needed to be masked with a protecting group until after metalation was achieved. As shown in the Supporting Information, using a benzyl protecting group with the starting material 4-OCH₂Ph-2,6-difluoropyridine led to 1^{OCH₂Ph} (following the method in Scheme 3), which then could be cleanly deprotected by hydrogenation with Pd on C in acetonitrile to produce 1^{OH}. Further experimental and full characterization details for all new compounds are shown in the Supporting Information.

Crystal Structures. The crystal structures for complexes 1^{Me}, 1^{NMe₂}, and 1^{OCH₂Ph} are shown in Figure 1. All of these complexes adopt a distorted-octahedral geometry with the CNC pincer occupying a meridional plane. Complex 1^{OH} was recrystallized from acetonitrile and diethyl ether, leading to a dimer with one molecular unit deprotonated (1^{OH} + 1^O), as shown in Figure 1. The OH-bearing pincer ligand is expected to be acidic, and thus this result is not surprising. For

Scheme 3. General Synthetic Procedure for $\mathbf{1}^R$ ^a

^aReagents and solvents: (a) 1*H*-imidazole, base, DMF; (b) methyl trifluoromethanesulfonate, DMF; (c) $[\text{Ru}(p\text{-cym})\text{Cl}_2]_2$, base, acetonitrile.

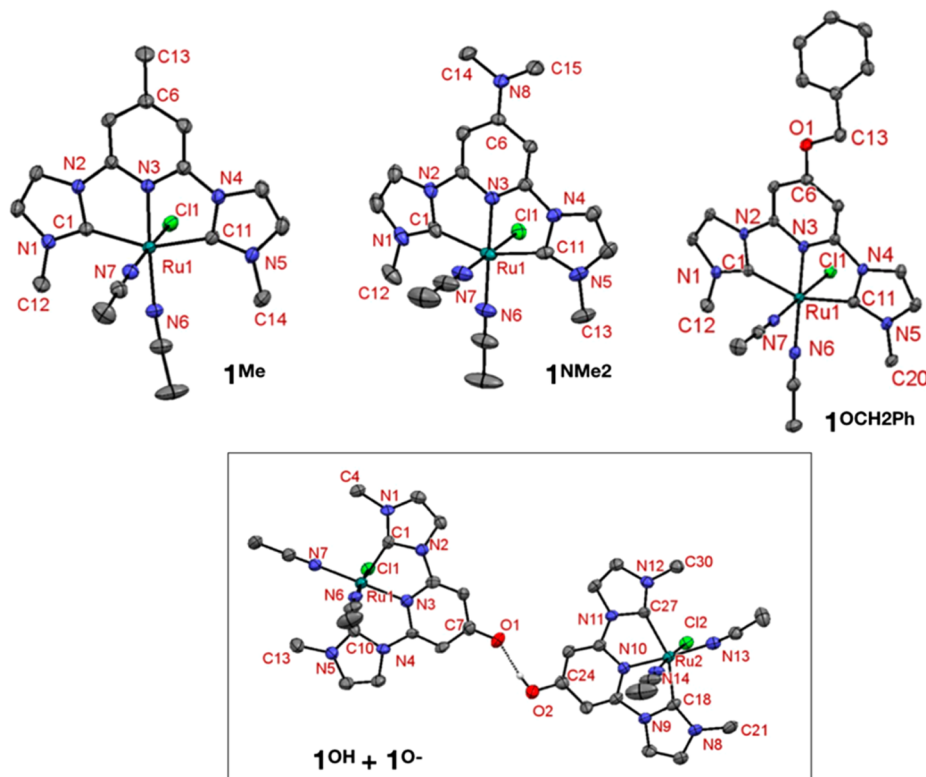


Figure 1. Molecular diagrams of complexes $\mathbf{1}^{\text{Me}}$, $\mathbf{1}^{\text{NMe}_2}$, $\mathbf{1}^{\text{OCH}_2\text{Ph}}$, and $(\mathbf{1}^{\text{OH}} + \mathbf{1}^{\text{O}^-})$ based on crystallographic data with most hydrogen atoms (except one in $(\mathbf{1}^{\text{OH}} + \mathbf{1}^{\text{O}^-})$) and counter-anions removed for clarity. Thermal ellipsoids are drawn at the 40% probability level.

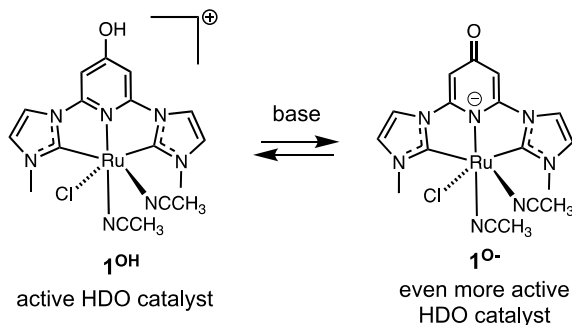
comparison, the same OH-bearing pincer ligand bound to Ni(II) exhibits a pK_a value of 5.4(4) in DMSO and was readily isolated in the O^- form.³⁰ The $\text{O}1\cdots\text{O}2$ distance of 2.540(8) Å reflects a strong hydrogen-bonding interaction.³² The $\text{C}_{\text{py}}-\text{O}$ distances reflect the charge on each pyridinol ring, with $\text{C}24-\text{O}2 = 1.35(1)$ Å for $\mathbf{1}^{\text{OH}}$ indicating some π donation into the ring (with a C–O bond order between single and double) and $\text{C}7-\text{O}1 = 1.29(1)$ Å for $\mathbf{1}^{\text{O}^-}$ indicating more $\text{C}=\text{O}$ character for the anionic pincer ring.

The structures of $\mathbf{1}^{\text{NMe}_2}$ and $\mathbf{1}^{\text{OCH}_2\text{Ph}}$ show the π donor effect of the pyridine substituent on the bond lengths in the pincer. The distances are $\text{C}6-\text{N}8 = 1.358(5)$ Å in $\mathbf{1}^{\text{NMe}_2}$ and $\text{C}6-\text{O}1 = 1.353(4)$ Å in $\mathbf{1}^{\text{OCH}_2\text{Ph}}$ which both reflect substantial $\text{C}=\text{X}$ double-bond character. Similarly, other methoxy-substituted pincers show C–O bond distances (1.34–1.36 Å) between single (~1.43 Å) and double (~1.23 Å) bond lengths.^{28,29} Furthermore, the C–C distances within the aromatic ring

show some loss of aromaticity with long C–C distances of ~1.42 Å and short C–C distances of ~1.36 Å for $\mathbf{1}^{\text{NMe}_2}$. This effect is strongest with NMe_2 as a strong π donor, and the effect is less pronounced for $\mathbf{1}^{\text{OCH}_2\text{Ph}}$. The other bond lengths and angles for these compounds are tabulated in the Supporting Information and are unremarkable.

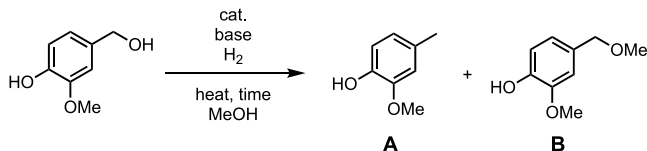
Spectroscopy Showing Acid–Base Reactions on $\mathbf{1}^{\text{OH}}$.

Since the catalysis results described below will use acid or base to control the protonation state of the pincer ligand, it is important to first describe the fundamental acid–base chemistry in the absence of substrate. Upon deprotonation of $\mathbf{1}^{\text{OH}}$ with Na_2CO_3 in CD_3OD , the ^1H NMR spectrum exhibits an upfield shift due to the formation of $\mathbf{1}^{\text{O}^-}$ (Scheme 4). The pyridine C–H protons exhibit the greatest shift from δ 6.97 ppm for $\mathbf{1}^{\text{OH}}$ to 6.58 ppm for $\mathbf{1}^{\text{O}^-}$. Upfield shifts were also seen for the imidazole-derived NHC ring protons. A similar

Scheme 4. Activation of Protic HDO Catalysts by Base

pattern was seen in the ^1H NMR for a Ni(II) complex bearing the same OH-containing pincer, with an upfield shift from δ 6.96 to 6.21 ppm upon deprotonation in DMSO- d_6 .³⁰ The magnitude of the change in chemical shift is likely sensitive to solvent effects. The IR data also support deprotonation of 1^{OH} with base, as there are several changes in the C=N stretching frequencies involving the pyridine ring. A peak at 1524 cm^{-1} is tentatively ascribed to a C=O stretch for $1^{\text{O}-}$, which is similar to the observed C=O stretch at 1568 cm^{-1} for a Ni(II) complex of the same pincer ligand.³⁰

Hydrodeoxygenation of Substrates. Vanillyl alcohol (VA) was used as a surrogate for lignin-derived monomers, and catalytic conversion of VA was carried out as shown in **Scheme 5**. For all catalysts and conditions studied, the catalytic reaction

Scheme 5. Catalytic Conversion of Vanillyl Alcohol Showing the Major Products Obtained^a

^a"cat." refers to the catalyst structures shown in **Scheme 2**.

yielded two major products labeled as **A** and **B** in **Scheme 5** and ring hydrogenation products were not observed. Product **A** (creosol) reduces the oxygen content of VA through the desired hydrodeoxygenation (HDO) reaction. Further reduction in the oxygen content of **A** was not observed in this work; specifically, we did not observe the HDO reaction on phenolic oxygen atoms. Product **B** (methyl vanillyl ether) is the alkylation product (Williamson ether synthesis) in methanol solvent and is considered an undesired product, as it does not reduce the oxygen content of VA. In fact, control experiments in which the transition-metal catalyst was omitted (**Table 1**, entries 18–20) illustrate that product **B** can be obtained readily as the major product by treating VA with methanol under hydrogen (290 psi) in the presence of base (44–84% yield) or acid (>99% yield). However, no significant yield of product **A** is obtained without a transition-metal catalyst (**Table 1**, entry 17).

A survey of the catalytic ability of the catalysts in **Scheme 2** was performed, and the results and reaction conditions are shown in **Table 1**. In entries 1–10, we first investigated the activity of all the catalysts in the *absence* of base. The catalysts of type 1^R are organized in order of decreasing yield of **A** (entries 1–5) with $R = \text{OH} > \text{OMe} > \text{NMe}_2 > \text{Me} > \text{H}$. While most of these catalysts (except 1^{H}) are competent at

Table 1. Screening Ruthenium Pincer Catalysts for Hydrodeoxygenation of Vanillyl Alcohol^a

entry	cat.	conversn (%) ^b	yield of A (%) ^c	yield of B (%) ^c
1	1^{OH}	91(1)	39.1(5)	52.2(8)
2	1^{OMe}	99.9(1)	30.7(4)	69.2(4)
3	1^{NMe_2}	93.6(2)	24.2(4)	69.4(3)
4	1^{Me}	99.5(4)	20.9(2)	78.6(4)
5	1^{H}	18.5(4)	15.0(4)	1.9(1)
6	2^{OMe}	100.0 ^d	16.8(5)	83.2(5)
7	2^{H}	99.9(1)	16.3(4)	83.7(4)
8	3	99.6(1)	21.4(7)	78.2(7)
9	4A	14(1)	2(2)	11(2)
10	4B	100.0 ^d	2.1(2)	97.9(2)
11 ^e	1^{OH}	98.0(4)	95.8(7)	0.2(1)
12 ^e	1^{OMe}	92(4)	88(5)	3(2)
13 ^e	1^{NMe_2}	91(4)	89(4)	1.6(3)
14 ^e	1^{Me}	79(3)	76(3)	1.8(4)
15 ^f	1^{NMe_2}	100.0 ^d	2(1)	98(1)
16 ^f	1^{Me}	99.9(1)	2.5(1)	97.4(1)
17	none	19.0(8)	1.8(4)	15.5(7)
18 ^g	none	45.9(4)	1.9(7)	43.6(6)
19 ^h	none	14(1)	3(1)	84(1)
20 ^f	none	100.0 ^d	0.16(9)	99.95(9)

^aAll experiments were done in triplicate and analyzed by GC. The estimated standard deviation in the last digit is reported in parentheses. Conditions: 0.0642 M vanillyl alcohol in methanol, 1 mol % of catalyst, 290 psi of H_2 , 100 °C for 1 h. See the Supporting Information for further details.

^bConversion is calculated on the basis of starting material consumption. ^cYield is calculated from the GC data. ^dQuantitative conversion was observed in all three experiments. ^e50 mol % of Na_2CO_3 was added. ^f1 mol % of HOTf was added. ^g10 mol % of Na_2CO_3 was added. ^h110 mol % of Na_2CO_3 was added.

accelerating the methylation of VA (**B** formation), it appears that the presence of a strong π -donor group on the pyridine ring is needed for the efficient hydrodeoxygenation and formation of product **A**. When catalysts of types 2 and 3 are considered next (entries 6–8), these catalysts are competent at the methylation of VA (78–84% yield of product **B**), but they fail to produce large yields of the HDO product **A** (16–21% yield). Furthermore, by a comparison of 1^{OMe} , 2^{OMe} , and 3, all of which bear methoxy groups on the pyridine rings, it is observed that the substitution of the imidazole-based NHC (1^{OMe}) for the benzimidazole-based NHC (2^{OMe} and 3) was detrimental, perhaps due to the weaker donor properties for the benzimidazole-derived NHC rings. Finally, catalysts 4A and 4B were tested (entries 9 and 10). Catalyst 4A is not competent at the methylation or the HDO reaction (cf. entry 17 in **Table 1**), and it seems reasonable to suggest that a lack of labile ligands on the Ru center is detrimental to the catalytic reaction. Catalyst 4B appears to serve as a Lewis acid for the effective methylation of VA, but it fails at the HDO reaction. Comparing 4B to 3 (2% vs 21% yield or A) would suggest that the addition of a bipy ligand is detrimental. This result suggests that multiple free sites are needed for the HDO reaction. Overall, entries 1–10 in **Table 1** illustrate that the presence of two labile ligands combined with electronic factors of the pincer ligand appear to enhance the HDO reaction with 1^{OH} as the best catalyst in **Scheme 2** under neutral conditions.

One catalyst (1^{NMe_2}) contains a basic group that can potentially be modified by the addition of external acids. However, triflic acid is detrimental to the HDO reaction in general, whether or not a basic group is present on the catalyst

structure (as in $\mathbf{1}^{\text{NMe}_2}$ and $\mathbf{1}^{\text{Me}}$ in entries 15 and 16, Table 1) because it promotes the formation of product B. These results are similar to entry 20 in Table 1, which shows the effect of triflic acid alone.

In relation to the above studies with HOTf, attempts to protonate $\mathbf{1}^{\text{NMe}_2}$ with HOTf did not lead to any substantial changes in the ^1H NMR spectrum in DMSO. Some slight changes were observed in the IR spectrum upon adding HOTf, but it is possible that these changes are due to hydrogen bonding with HOTf or H_3O^+ formed from adventitious water or incomplete protonation. While the pK_a value of the conjugate acid of 4-dimethylaminopyridine (DMAP) is 9.6 in water³³ and DMAP would be protonated readily by HOTf, it is possible that $\mathbf{1}^{\text{NMe}_2}$ is less basic than DMAP due to delocalization of the lone pair on NMe_2 into the pyridine ring. In fact, the crystal structure above for $\mathbf{1}^{\text{NMe}_2}$ suggests that there is substantial double-bond character for $\text{C}=\text{NMe}_2$.

External base serves to promote the HDO reaction with several catalysts. Entry 11 (Table 1) shows that the presence of base (50 mol % of Na_2CO_3) with $\mathbf{1}^{\text{OH}}$ facilitated the HDO reaction and led to a 96% yield for product A in just 1 h. Thus, nearly complete conversion to A is obtained by deprotonating $\mathbf{1}^{\text{OH}}$, which enhances the π -donor properties of the pincer ligand (Scheme 4). The addition of base to $\mathbf{1}^{\text{OMe}}$, $\mathbf{1}^{\text{NMe}_2}$, and $\mathbf{1}^{\text{Me}}$ was also explored. The base should not affect the structures of $\mathbf{1}^{\text{OMe}}$, $\mathbf{1}^{\text{NMe}_2}$, or $\mathbf{1}^{\text{Me}}$; thus, any changes in the observed reactivity would not be attributed to changes in the catalyst. As illustrated by entry 12 of Table 1, the use of base with $\mathbf{1}^{\text{OMe}}$ generates an 88% yield of A, showing that base accelerates the HDO reaction even in the absence of a protic ligand (cf. entry 2 with a 31% yield of A). A base also enhances catalysis with $\mathbf{1}^{\text{NMe}_2}$, and an 89% yield (entry 13) of the HDO product A is obtained (vs 24% without base, entry 3). Similarly, adding base to $\mathbf{1}^{\text{Me}}$ leads to an increased yield of A (76% in entry 14) but a somewhat decreased percent conversion. Comparing these results shows that the selectivity to the desired product is increased with base present for all four catalysts: $\mathbf{1}^{\text{R}}$ where R = OH, OMe, NMe₂, Me. However, base alone does not lead to the desired product A (entries 18 and 19, Table 1). Hydrogen activation most likely occurs via the well-established reaction $\text{Ru} + \text{H}_2 \rightarrow \text{Ru}-\text{H} + \text{H}^+$. The generation of H^+ is detrimental to the reaction selectivity, likely by promoting the formation of the undesired product B. Thus, the base can play two roles: it can prevent acid buildup and undesired pathways and, when the catalyst is designed properly, the base can further activate the catalyst to favor formation of A vs B. Accordingly, $\mathbf{1}^{\text{OH}}$ with base is our most selective catalyst, with an A:B ratio of 479:1. The other catalysts ($\mathbf{1}^{\text{OMe}}$, $\mathbf{1}^{\text{NMe}_2}$, $\mathbf{1}^{\text{Me}}$) do not come close to this selectivity, with at best 57:1.

With the knowledge in hand that base is advantageous to the reaction and that catalyst $\mathbf{1}^{\text{OH}}$ can be further activated by base, the experimental conditions were systematically varied to further enhance catalytic activity. Increasing the reaction temperature did not have a significant effect on reaction selectivity or activity (see the Supporting Information for details). In addition, catalyst decomposition was observed at temperatures $>150^\circ\text{C}$. Next, the identity and loading of the base was explored (Table 2). Strong bases such as NaOH and $\text{NaO}^{\text{t}}\text{Bu}$ were detrimental to the reaction (entries 1 and 2). Weak bases such as Na_2CO_3 gave optimal conversion and selectivity at high base loadings (entries 4–9). The use of a very weak base (NaHCO_3 , entry 3) did not lead to good

Table 2. Hydrodeoxygenation of Vanillyl Alcohol with $\mathbf{1}^{\text{OH}}$: Evaluating the Identity and Quantity of Base^a

entry	base (mol %)	conversion (%) ^b	yield of A (%) ^c	yield of B (%) ^c
1	$\text{NaO}^{\text{t}}\text{Bu}$ (10)	41.6(4)	38.1(4)	1.65(6)
2	NaOH (10)	50.8(8)	47(1)	2.1(1)
3	NaHCO_3 (10)	29.2(8)	27(1)	0.6(2)
4	K_2CO_3 (10)	51.1(5)	46.8(6)	0.8(6)
5	Na_2CO_3 (11)	20(2)	16(2)	0.5(2)
6	Na_2CO_3 (10)	51(2)	48(2)	1.1(2)
7	Na_2CO_3 (25)	73(1)	69.5(4)	2(1)
8	Na_2CO_3 (50)	98.0(4)	95.8(7)	0.2(1)
9	Na_2CO_3 (110)	99.73(6)	98.8(3)	0.4(3)

^aAll experiments were done in triplicate and were analyzed by GC. Conditions: 0.0642 M vanillyl alcohol in methanol, 1 mol % of $\mathbf{1}^{\text{OH}}$, 290 psi of H_2 , 100°C for 1 h. See the Supporting Information for further details. ^bConversion is calculated on the basis of starting material consumption. ^cYield is calculated from the GC data.

conversion. Thus, the ideal conditions (50 or 110 mol % of Na_2CO_3 and 1 mol % of $\mathbf{1}^{\text{OH}}$) led to selective and nearly complete formation of A. Using these optimal conditions (50 mol % of Na_2CO_3), we also explored the hydrodeoxygenation of less activated substrates, but we see that $\mathbf{1}^{\text{OH}}$ (1 mol %) is not effective at converting benzyl alcohol to toluene (see the Supporting Information for details).

Xu et al. have investigated the role of pH, promoters (e.g., formic acid), and remote directing groups in the HDO reaction of a variety of alcohols and observed optimum yields at pH 1.6 in water. They propose an $\text{S}_{\text{N}}1$ mechanism with OH_2 loss from substrate followed by hydride transfer from the catalyst to the substrate.³⁴ Formic acid served as a source of protons to modulate pH, and the resulting formate was decarboxylated to produce an iridium hydride catalyst. In our case, increased HDO reactivity is observed with a weak base present, which suggests that a different mechanism is operative in our study. There appears to be an optimum balance for base strength in our case. Sodium carbonate is strong enough to facilitate catalyst deprotonation but does not generate any species capable of direct binding to the active Ru centers of our catalysts. Conversely, bases such as $\text{NaO}^{\text{t}}\text{Bu}$ and NaOH both generate species that may bind to the Ru centers and inhibit catalysis; these species include *tert*-butoxide, hydroxide, and methoxide from solvent deprotonation.

As described in the Supporting Information, exploring product B as a substrate and under optimal catalytic conditions (with $\mathbf{1}^{\text{OH}}$ or $\mathbf{1}^{\text{OMe}}$ as the catalyst) led to slower formation of A in comparison to the conversion of VA directly to A. In view of our data, we propose that product B formation does not facilitate the formation of A. This suggests two possibilities. (1) Perhaps B must be converted to VA by any adventitious water present before the HDO reaction can occur. (2) Alternatively, B goes directly to A, but by a mechanism that is different from that employed when we start with VA and it must be inherently slower. The methylated substrate B certainly cannot bind to ruthenium as readily as VA.

Once the optimum base loadings were established, a lower catalyst loading of $\mathbf{1}^{\text{OH}}$ was investigated to probe whether the catalyst can operate efficiently under very dilute conditions. Without an increase in the reaction time beyond 1 h, the lowest catalyst loading that results in quantitative conversion to product A is 0.05 mol % (Na_2CO_3 2.5 mol %, $T = 150^\circ\text{C}$, TON = 2000). When the temperature is lowered to 100°C ,

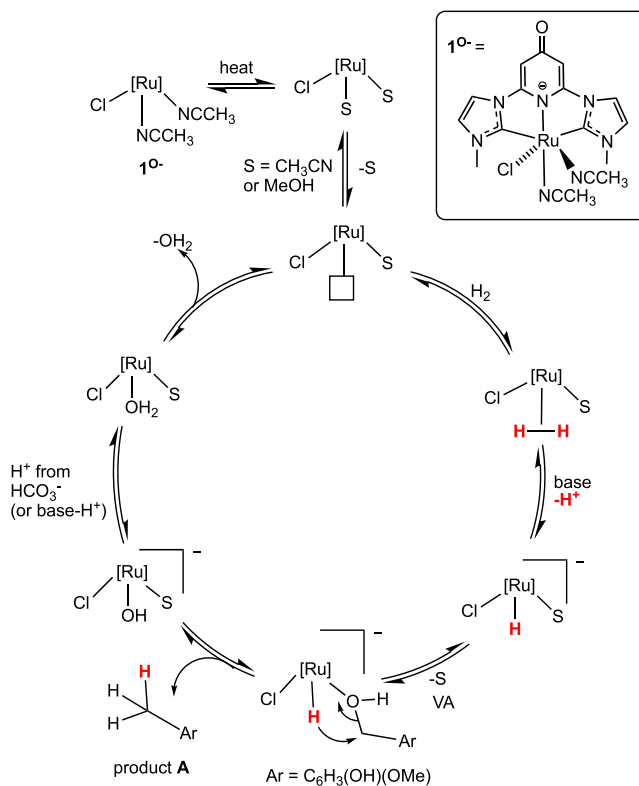
quantitative conversion can be obtained with 0.01 mol % catalyst loading in 3 days (Na_2CO_3 , 0.5 mol %, TON = 10000). Delightfully, this increases the turnover number 5-fold, and it may be further increased at either lower catalyst loadings or longer reaction times. Catalyst $\mathbf{1}^{\text{OH}}$ performs better than heterogeneous catalysts in the literature, which only achieve 90% yield of product A²¹ or which achieve similar results (>99% yield of A and selectivity) but only at much higher (e.g., 5 wt % for Zn/Pd/C) catalyst loadings.^{25,26}

For every catalytic system, there is a need to interrogate whether the active catalyst is homogeneous or heterogeneous in nature. To probe this issue for $\mathbf{1}^{\text{OH}}$, we performed the mercury test, since mercury is known to coat the surface of nanoparticles and typically results in lower activity for such heterogeneous systems.^{35–37} When we repeated entry 8 of Table 2 with a few drops of mercury added to the reaction vessel, we obtained 95% yield of A by GC (done in triplicate). Within experimental error, this result is the same as that for entry 8, and thus mercury does not alter the catalytic activity of $\mathbf{1}^{\text{OH}}$ with 50 mol % of Na_2CO_3 at 100 °C. This suggests that the catalyst is homogeneous and molecular under these conditions, though we caution that the nature of the true catalyst in solution is often sensitive to the specific conditions employed.^{38,39} Similarly, since catalyst $\mathbf{1}^{\text{OMe}}$ with 50 mol % of Na_2CO_3 present (entry 12, Table 1) showed a large run to run variation in results, we performed the mercury test on this system as well and obtained similar results (91(4)% conversion, 88(4)% yield of A, 2(1)% yield of B). This suggests that the variation seen is not due to nanoparticle formation for $\mathbf{1}^{\text{OMe}}$ with base.

Thus, with the data obtained herein we can propose a mechanism for the HDO reaction as catalyzed by $\mathbf{1}^{\text{O}^-}$ (Scheme 6). ^1H NMR data on $\mathbf{1}^{\text{OH}}$ mixed with Na_2CO_3 in CD_3OD supports the formation of $\mathbf{1}^{\text{O}^-}$, and slowly over 20 h at room temperature the exchange of acetonitrile ligands for solvent occurs (see the Supporting Information). This exchange should be much faster at 100 °C under our typical HDO conditions. This would be followed by the binding of H_2 to a free site by most likely displacing the solvent *trans* to the pyridine nitrogen. Here a π -donor ligand should help to increase the acidity of the transient dihydrogen complex via a more electron rich metal which donates into the σ^* orbital on bound H_2 .^{40,41} This serves to weaken or break the H–H bond (perhaps forming a dihydride intermediate), and then this complex can be deprotonated by base to form a metal hydride. In fact, both experimental and computational studies support that π -donor groups para to nitrogen on a pyridine ring can accelerate (de)hydrogenation reactions.^{42–47} (As an aside, the rate of formation and the stability of this metal hydride should be much less under acidic conditions, thus explaining why triflic acid inhibits the formation of A in our studies.)

Next, we propose that VA displaces the solvent and binds to the metal. The hydride can then attack the benzylic position to produce product A and a metal-bound hydroxide ligand. We cannot rule out an outer-sphere mechanism, in which hydride attacks VA in solution, but the need for multiple free sites suggests an inner-sphere mechanism. Release of water or hydroxide can allow the catalyst to begin another cycle. These steps may occur in a different order, or perhaps chloride loss occurs at some point during catalysis (binding H_2 is often faster at cationic and electron-deficient metal centers).⁴⁸ Additionally, while the phenolic protons of VA are more

Scheme 6. Mechanistic Proposal for Hydrodeoxygenation of Vanillyl Alcohol with Ruthenium Pincer Complexes^a



^aThe CNC pincer is represented as [Ru] here.

acidic and coordination of the phenolic O^- to the metal center may occur, this does not lead to products due to the inherent challenges in performing a substitution reaction on an sp^2 carbon (no HDO reaction on phenolic OH groups was observed herein). Furthermore, the presence of OH and OMe groups on the aromatic ring in VA serve to activate the benzylic position and may explain the reactivity at this site (vs a lack of reactivity for benzyl alcohol).³⁴

CONCLUSIONS

In this study, the electronic properties of ruthenium pincer complexes along with the ability to provide free sites for substrate binding were related to the ability for these complexes to function as HDO catalysts. At least one labile site was necessary for any catalytic activity (e.g., for formation of the methylation product, B) to be observed. Two to three labile ligand sites, however, proved necessary but not sufficient for good yields of the HDO product A. The best yields and selectivity for A were achieved with the most electron rich pincer ligand ($\mathbf{1}$ rather than 2 or 3) with π -donor substituents ($\mathbf{1}^{\text{NMe}_2}$, $\mathbf{1}^{\text{OMe}}$, $\mathbf{1}^{\text{OH}}$) in the presence of a weak base (Na_2CO_3). At low catalyst loadings (0.01 mol %), $\mathbf{1}^{\text{OH}}$ in the presence of base serves as a homogeneous catalyst that is able to achieve quantitative and selective conversion of vanillyl alcohol to the desired HDO product, A. With this knowledge in hand, we can design the next generation of homogeneous catalysts with increased reactivity toward all of the oxygenated sites on lignin-derived monomers.

■ ASSOCIATED CONTENT

SI Supporting Information

The Supporting Information is available free of charge at <https://pubs.acs.org/doi/10.1021/acs.organomet.9b00816>.

Experimental details on the synthesis and characterization of all compounds, optimization data, hydrodeoxygenation of various substrates, and control experiments ([PDF](#))

Accession Codes

CCDC 1981237–1981240 contain the supplementary crystallographic data for this paper. These data can be obtained free of charge via www.ccdc.cam.ac.uk/data_request/cif, or by emailing data_request@ccdc.cam.ac.uk, or by contacting The Cambridge Crystallographic Data Centre, 12 Union Road, Cambridge CB2 1EZ, UK; fax: +44 1223 336033.

■ AUTHOR INFORMATION

Corresponding Authors

Aaron K. Vannucci — Department of Chemistry and Biochemistry, University of South Carolina, Columbia, South Carolina 29208, United States;  orcid.org/0000-0003-0401-7208; Email: vannucci@mailbox.sc.edu

Elizabeth T. Papish — Department of Chemistry and Biochemistry, University of Alabama, Tuscaloosa, Alabama 35487, United States;  orcid.org/0000-0002-7937-8019; Email: etpapish@ua.edu

Authors

Wenzhi Yao — Department of Chemistry and Biochemistry, University of Alabama, Tuscaloosa, Alabama 35487, United States;  orcid.org/0000-0002-4874-0169

Sanjit Das — Department of Chemistry and Biochemistry, University of Alabama, Tuscaloosa, Alabama 35487, United States

Nicholas A. DeLucia — Department of Chemistry and Biochemistry, University of South Carolina, Columbia, South Carolina 29208, United States

Fengrui Qu — Department of Chemistry and Biochemistry, University of Alabama, Tuscaloosa, Alabama 35487, United States;  orcid.org/0000-0002-9975-2573

Chance M. Boudreaux — Department of Chemistry and Biochemistry, University of Alabama, Tuscaloosa, Alabama 35487, United States;  orcid.org/0000-0003-1322-9878

Complete contact information is available at:

<https://pubs.acs.org/doi/10.1021/acs.organomet.9b00816>

Notes

The authors declare the following competing financial interest(s): E.T.P. and A.K.V. are filing a patent application related to this work.

■ ACKNOWLEDGMENTS

We thank the NSF (CHE-1800214) for funding this research. We thank NSF CHE MRI 1828078 and UA for purchase of the SC XRD instrument. Preliminary data was also obtained with NSF OIA-1539035 support. S.D. thanks the University of Alabama's Graduate Council Fellowship (GCF). C. M. B. thanks AL EPSCoR for a graduate fellowship. The support of the National Science Foundation through the EPSCoR R-II Track-2 grant number OIA-1539105 is gratefully acknowledged by A.K.V.

■ REFERENCES

- (1) US_Energy_Information_Administration International Energy Outlook 2017. [https://www.eia.gov/outlooks/ieo/pdf/0484\(2017\).pdf](https://www.eia.gov/outlooks/ieo/pdf/0484(2017).pdf) (accessed 9/11/19).
- (2) Renewable_Energy_Policy_Network_for_21st_Century Renewables 2014 Global Status Report. https://www.ren21.net/wp-content/uploads/2019/05/GSR2014_Full-Report_English.pdf (accessed 9/11/2019).
- (3) Bridgwater, A. V. Renewable fuels and chemicals by thermal processing of biomass. *Chem. Eng. J.* **2003**, *91* (2), 87–102.
- (4) Raymundo, L. M.; Mullen, C. A.; Strahan, G. D.; Boateng, A. A.; Trierweiler, J. O. Deoxygenation of Biomass Pyrolysis Vapors via in Situ and ex Situ Thermal and Biochar Promoted Upgrading. *Energy Fuels* **2019**, *33* (3), 2197–2207.
- (5) Rahimi, A.; Ulbrich, A.; Coon, J. J.; Stahl, S. S. Formic-acid-induced depolymerization of oxidized lignin to aromatics. *Nature* **2014**, *515*, 249.
- (6) Huang, X.; Atay, C.; Korányi, T. I.; Boot, M. D.; Hensen, E. J. M. Role of Cu–Mg–Al Mixed Oxide Catalysts in Lignin Depolymerization in Supercritical Ethanol. *ACS Catal.* **2015**, *5* (12), 7359–7370.
- (7) Gasser, C. A.; Čvančarová, M.; Ammann, E. M.; Schäffer, A.; Shahgaldian, P.; Corvini, P. F.-X. Sequential lignin depolymerization by combination of biocatalytic and formic acid/formate treatment steps. *Appl. Microbiol. Biotechnol.* **2017**, *101* (6), 2575–2588.
- (8) Partenheimer, W. The Aerobic Oxidative Cleavage of Lignin to Produce Hydroxyaromatic Benzaldehydes and Carboxylic Acids via Metal/Bromide Catalysts in Acetic Acid/Water Mixtures. *Adv. Synth. Catal.* **2009**, *351* (3), 456–466.
- (9) Renders, T.; Van den Bosch, S.; Koelewijn, S. F.; Schutyser, W.; Sels, B. F. Lignin-first biomass fractionation: the advent of active stabilisation strategies. *Energy Environ. Sci.* **2017**, *10* (7), 1551–1557.
- (10) Das, A.; Rahimi, A.; Ulbrich, A.; Alherech, M.; Motagamwala, A. H.; Bhalla, A.; da Costa Sousa, L.; Balan, V.; Dumesic, J. A.; Hegg, E. L.; Dale, B. E.; Ralph, J.; Coon, J. J.; Stahl, S. S. Lignin Conversion to Low-Molecular-Weight Aromatics via an Aerobic Oxidation-Hydrolysis Sequence: Comparison of Different Lignin Sources. *ACS Sustainable Chem. Eng.* **2018**, *6* (3), 3367–3374.
- (11) Gollakota, A. R. K.; Reddy, M.; Subramanyam, M. D.; Kishore, N. A review on the upgradation techniques of pyrolysis oil. *Renewable Sustainable Energy Rev.* **2016**, *58* (C), 1543–1568.
- (12) Luo, H.; Abu-Omar, M. M. Lignin extraction and catalytic upgrading from genetically modified poplar. *Green Chem.* **2018**, *20* (3), 745–753.
- (13) Nolte, M. W.; Shanks, B. H. A Perspective on Catalytic Strategies for Deoxygenation in Biomass Pyrolysis. *Energy Technology* **2017**, *5* (1), 7–18.
- (14) Zakzeski, J.; Bruijnincx, P. C. A.; Jongerius, A. L.; Weckhuysen, B. M. The Catalytic Valorization of Lignin for the Production of Renewable Chemicals. *Chem. Rev.* **2010**, *110* (6), 3552–3599.
- (15) Shao, Y.; Xia, Q.; Dong, L.; Liu, X.; Han, X.; Parker, S. F.; Cheng, Y.; Daemen, L. L.; Ramirez-Cuesta, A. J.; Yang, S.; Wang, Y. Selective production of arenes via direct lignin upgrading over a niobium-based catalyst. *Nat. Commun.* **2017**, *8* (1), 16104.
- (16) Guo, T.; Xia, Q.; Shao, Y.; Liu, X.; Wang, Y. Direct deoxygenation of lignin model compounds into aromatic hydrocarbons through hydrogen transfer reaction. *Appl. Catal., A* **2017**, *547*, 30–36.
- (17) Baddour, F. G.; Witte, V. A.; Nash, C. P.; Griffin, M. B.; Ruddy, D. A.; Schaidle, J. A. Late-Transition-Metal-Modified β -Mo₂C Catalysts for Enhanced Hydrogenation during Guaiacol Deoxygenation. *ACS Sustainable Chem. Eng.* **2017**, *5* (12), 11433–11439.
- (18) Hsu, P.-J.; Jiang, J.-W.; Lin, Y.-C. Does a Strong Oxophilic Promoter Enhance Direct Deoxygenation? A Study of NiFe, NiMo, and NiW Catalysts in p-Cresol Conversion. *ACS Sustainable Chem. Eng.* **2018**, *6* (1), 660–667.
- (19) Ju, C.; Li, M.; Fang, Y.; Tan, T. Efficient hydro-deoxygenation of lignin derived phenolic compounds over bifunctional catalysts with optimized acid/metal interactions. *Green Chem.* **2018**, *20* (19), 4492–4499.

- (20) Song, W.; Zhou, S.; Hu, S.; Lai, W.; Lian, Y.; Wang, J.; Yang, W.; Wang, M.; Wang, P.; Jiang, X. Surface Engineering of CoMoS Nanosulfide for Hydrodeoxygenation of Lignin-Derived Phenols to Arenes. *ACS Catal.* **2019**, *9* (1), 259–268.
- (21) Hao, P.; Schwartz, D. K.; Medlin, J. W. Effect of Surface Hydrophobicity of Pd/Al₂O₃ on Vanillin Hydrodeoxygenation in a Water/Oil System. *ACS Catal.* **2018**, *8* (12), 11165–11173.
- (22) Lien, C.-H.; Medlin, J. W. Promotion of Activity and Selectivity by Alkanethiol Monolayers for Pd-Catalyzed Benzyl Alcohol Hydrodeoxygenation. *J. Phys. Chem. C* **2014**, *118* (41), 23783–23789.
- (23) Parsell, T. H.; Owen, B. C.; Klein, I.; Jarrell, T. M.; Marcum, C. L.; Haupert, L. J.; Amundson, L. M.; Kenttämaa, H. I.; Ribeiro, F.; Miller, J. T.; Abu-Omar, M. M. Cleavage and hydrodeoxygenation (HDO) of C–O bonds relevant to lignin conversion using Pd/Zn synergistic catalysis. *Chem. Sci.* **2013**, *4* (2), 806–813.
- (24) Liu, H.; Jiang, T.; Han, B.; Liang, S.; Zhou, Y. Selective Phenol Hydrogenation to Cyclohexanone Over a Dual Supported Pd–Lewis Acid Catalyst. *Science* **2009**, *326*, 1250–1252.
- (25) DeLucia, N. A.; Das, N.; Overa, S.; Paul, A.; Vannucci, A. K. Low temperature selective hydrodeoxygenation of model lignin monomers from a homogeneous palladium catalyst. *Catal. Today* **2018**, *302*, 146–150.
- (26) DeLucia, N. A.; Jystad, A.; Laan, K. V.; Tengco, J. M. M.; Caricato, M.; Vannucci, A. K. Silica Supported Molecular Palladium Catalyst for Selective Hydrodeoxygenation of Aromatic Compounds under Mild Conditions. *ACS Catal.* **2019**, *9*, 9060–9071.
- (27) Rodrigues, R. R.; Boudreux, C. M.; Papish, E. T.; Delcamp, J. H. Photocatalytic Reduction of CO₂ to CO and Formate: Do Reaction Conditions or Ruthenium Catalysts Control Product Selectivity? *ACS Appl. Energy Mater.* **2019**, *2*, 37–46.
- (28) Das, S.; Rodrigues, R. R.; Lamb, R. W.; Qu, F.; Reinheimer, E.; Boudreux, C. M.; Webster, C. E.; Delcamp, J. H.; Papish, E. T. Highly Active Ruthenium CNC Pincer Photocatalysts for Visible-Light-Driven Carbon Dioxide Reduction. *Inorg. Chem.* **2019**, *58* (12), 8012–8020.
- (29) Boudreux, C. M.; Liyanage, N. P.; Shirley, H.; Siek, S.; Gerlach, D. L.; Qu, F.; Delcamp, J. H.; Papish, E. T. Ruthenium(II) complexes of pyridinol and N-heterocyclic carbene derived pincers as robust catalysts for selective carbon dioxide reduction. *Chem. Commun.* **2017**, *53*, 11217–11220.
- (30) Burks, D. B.; Davis, S.; Lamb, R. W.; Liu, X.; Rodrigues, R. R.; Liyanage, N. P.; Sun, Y.; Webster, C. E.; Delcamp, J. H.; Papish, E. T. Nickel(II) pincer complexes demonstrate that the remote substituent controls catalytic carbon dioxide reduction. *Chem. Commun.* **2018**, *54*, 3819–3822.
- (31) Grader, C.; Krahmer, J.; Sönnichsen, F. D.; Näther, C.; Tuczek, F. Molybdenum(0)–carbonyl complexes supported by mixed benzimidazol-2-ylidene/phosphine ligands: Influence of benzannulation on the donor properties of the NHC groups. *J. Organomet. Chem.* **2014**, *770*, 61–68.
- (32) Jeffrey, G. A. Hydrogen-Bonding: An update. *Crystallogr. Rev.* **2003**, *9* (2), 135–176.
- (33) Kaljurand, I.; Kütt, A.; Sooväli, L.; Rodima, T.; Määmets, V.; Leito, I.; Koppel, I. A. Extension of the Self-Consistent Spectrophotometric Basicity Scale in Acetonitrile to a Full Span of 28 pKa Units: Unification of Different Basicity Scales. *J. Org. Chem.* **2005**, *70* (3), 1019–1028.
- (34) Yang, S.; Tang, W.; Yang, Z.; Xu, J. Iridium-Catalyzed Highly Efficient and Site-Selective Deoxygenation of Alcohols. *ACS Catal.* **2018**, *8* (10), 9320–9326.
- (35) Anton, D. R.; Crabtree, R. H. Dibenzo[a,e]cyclooctatetraene in a proposed test for heterogeneity in catalysts formed from soluble platinum-group metal complexes. *Organometallics* **1983**, *2* (7), 855–859.
- (36) Widegren, J. A.; Bennett, M. A.; Finke, R. G. Is It Homogeneous or Heterogeneous Catalysis? Identification of Bulk Ruthenium Metal as the True Catalyst in Benzene Hydrogenations Starting with the Monometallic Precursor, Ru(II)(η⁶-C₆Me₆)(OAc)₂, Plus Kinetic Characterization of the Heterogeneous Nucleation, Then Autocatalytic Surface-Growth Mechanism of Metal Film Formation. *J. Am. Chem. Soc.* **2003**, *125* (34), 10301–10310.
- (37) Eberhard, M. R. Insights into the Heck Reaction with PCP Pincer Palladium(II) Complexes. *Org. Lett.* **2004**, *6* (13), 2125–2128.
- (38) Stracke, J. J.; Finke, R. G. Water Oxidation Catalysis Beginning with 2.5 μM [Co 4(H₂O) 2(PW 9O 34) 2] 10–: Investigation of the True Electrochemically Driven Catalyst at ≥ 600 mV Overpotential at a Glassy Carbon Electrode. *ACS Catal.* **2013**, *3*, 1209–1219.
- (39) Bayram, E.; Linehan, J. C.; Fulton, J. L.; Roberts, J. A. S.; Szymczak, N. K.; Smurthwaite, T. D.; Özkar, S.; Balasubramanian, M.; Finke, R. G. Is It Homogeneous or Heterogeneous Catalysis Derived from [RhCp*Cl₂]²⁻? In Operando XAFS, Kinetic, and Crucial Kinetic Poisoning Evidence for Subnanometer Rh₄ Cluster-Based Benzene Hydrogenation Catalysis. *J. Am. Chem. Soc.* **2011**, *133* (46), 18889–18902.
- (40) Kristjánsdóttir, S. S.; Norton, J. R. *Acidity of Hydrido Transition Metal Complexes in Solution*; VCH: 1992; Chapter 9.
- (41) Papish, E. T.; Magee, M. P.; Norton, J. R. Protonation of transition metal hydrides to give dihydrogen complexes. Mechanistic implications and catalytic applications. In *Recent Advances in Hydride Chemistry*; Elsevier: 2001; pp 39–74.
- (42) Cho, D.; Ko, K. C.; Lee, J. Y. Catalytic Mechanism for the Ruthenium-Complex-Catalyzed Synthesis of Amides from Alcohols and Amines: A DFT Study. *Organometallics* **2013**, *32* (16), 4571–4576.
- (43) Hull, J. F.; Himeda, Y.; Wang, W.-H.; Hashiguchi, B.; Periana, R.; Szalda, D. J.; Muckerman, J. T.; Fujita, E. Reversible hydrogen storage using CO₂ and a proton-switchable iridium catalyst in aqueous media under mild temperatures and pressures. *Nat. Chem.* **2012**, *4* (5), 383–388.
- (44) Wang, W.-H.; Hull, J. F.; Muckerman, J. T.; Fujita, E.; Himeda, Y. Second-Coordination-Sphere and Electronic Effects Enhance Iridium(III)-Catalyzed Homogeneous Hydrogenation of Carbon Dioxide in Water Near Ambient Temperature And Pressure. *Energy Environ. Sci.* **2012**, *5* (7), 7923–7926.
- (45) Himeda, Y.; Onozawa-Komatsuzaki, N.; Sugihara, H.; Kasuga, K. Simultaneous Tuning of Activity and Water Solubility of Complex Catalysts by Acid–Base Equilibrium of Ligands for Conversion of Carbon Dioxide. *Organometallics* **2007**, *26* (3), 702–712.
- (46) Himeda, Y. Conversion of CO₂ into Formate by Homogeneously Catalyzed Hydrogenation in Water: Tuning Catalytic Activity and Water Solubility through the Acid–Base Equilibrium of the Ligand. *Eur. J. Inorg. Chem.* **2007**, *2007* (25), 3927–3941.
- (47) Sandhya, K. S.; Remya, G. S.; Suresh, C. H. Pincer Ligand Modifications To Tune the Activation Barrier for H₂ Elimination in Water Splitting Milstein Catalyst. *Inorg. Chem.* **2015**, *54* (23), 11150–11156.
- (48) Crabtree, R. Iridium compounds in catalysis. *Acc. Chem. Res.* **1979**, *12* (9), 331–337.